Electronic Supplementary Material (ESI) for Journal of Materials Chemistry

Electronic Supporting Information for

Succinic Anhydrides Functionalized Alkenoic Ligands: A Facile Route to Synthesize Water Dispersible Nanocrystals

*Erwin Peng, Jun Ding and Jun Min Xue**

Department of Materials Science & Engineering, Faculty of Engineering, National University of Singapore (NUS), 7 Engineering Drive 1, Singapore 117574.

S1. Maleinization of Oleic Acid

The unsaturated fatty acid maleinization reaction was adopted according to the well documented procedures of synthesizing the alkenyl succinic anhydrides (ASA) that are often used in industry (i.e. for paper sizing agents and cutting fluids lubricants) [1]. For monounsaturated fatty acid such as oleic acid, 1-3 times of maleic anhydride to oleic acid molar ratio are recommended to obtain high yield of maleinized oleic acid adducts [2]. Typical maleinization of oleic acid reaction is carried out under inert static nitrogen gas condition without the presence of any solvent or catalyst. There were several reported reaction conditions whereby xylenes [1c] and transition metal [3] solvent/catalyst were used to improve the yield of the maleinization reaction. For our proposed applications whereby maleinization reaction is combined with thermolysis reactions, the presence of other solvent or catalyst would complicate the overall synthesis reactions. Thus, in this report, we do not consider any addition of catalyst.

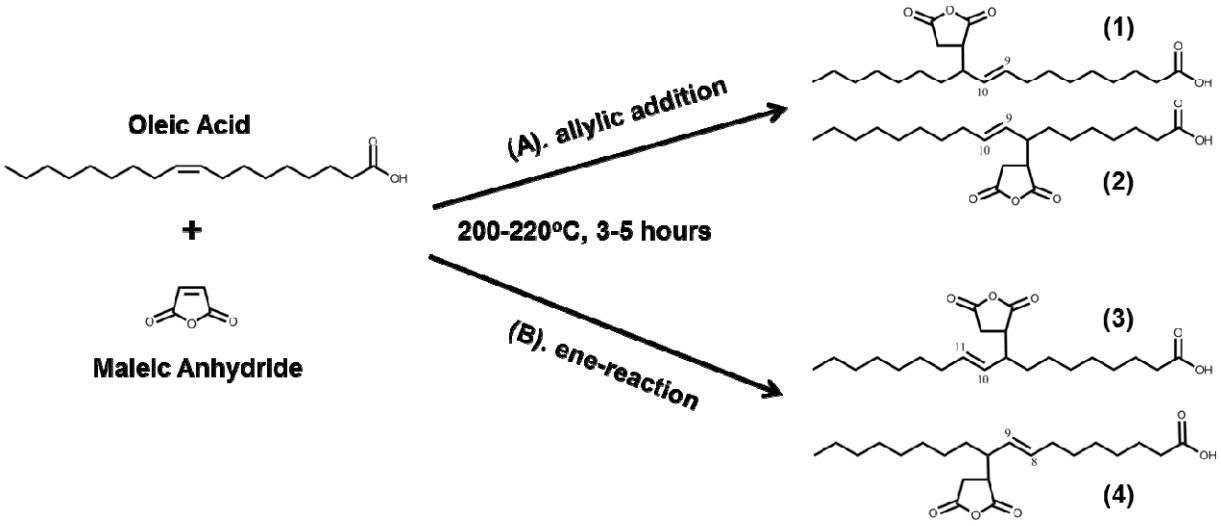

Fig.S1 Schematic of oleic acid maleinization reaction. The maleinization reaction proceeds through two different pathways that involve the mono unsaturated double bond (adopted from Ref [3a])

Even though the maleinization of oleic acid reaction and its subsequent applications have been widely documented in the literature, there is little information about the exact reaction mechanism. As illustrated

in **Fig.S1**, there are two commonly proposed reaction pathways which could possibly occur during the maleinization process which are widely accepted currently: (1) ene-reaction and (2) the addition in allylic position. Both reaction mechanisms would favour the attachment of the succinic anhydride functional groups on either side of the alkenyl functional groups [1]. Regardless of the reaction pathway all maleinized oleic acid product should bear a succinic anhydride functional groups and therefore it can be dispersed into aqueous phase once hydrolysed. To avoid confusion, succinic anhydride terminology would be used to denote maleic anhydride functional groups that have been grafted onto oleic acid.

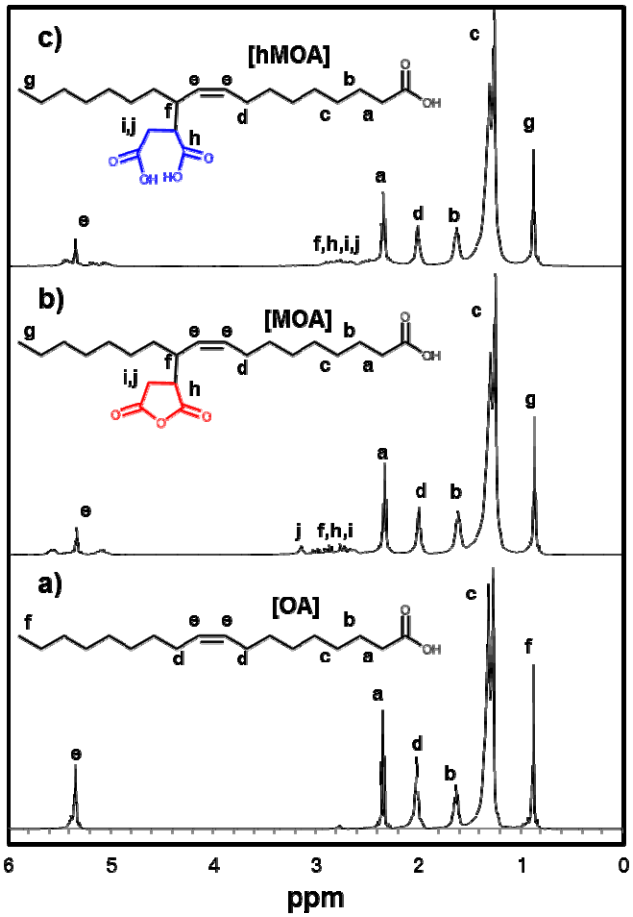

Fig.S2 ^{1}H-NMR spectra of (a) pure oleic acid (OA), (b) maleinized oleic acid (MOA) and (c) hydrolysed MOA (hMOA) in CDCl3 (400MHz, 1H δ: 7.27 ppm). Chemical shifts for OA, MOA and hMOA are reported in parts-per-million δ.

To confirm the maleinization reaction and the potential conversion of its hydrophobic adduct to hydrophilic analogue, we carried out a preliminary study by simply reacting maleic anhydride with oleic acid (OA) at 210^{o}C for 4 hours under static nitrogen environment. The reaction was carried out in a three-neck round bottom flask equipped with condenser and magnetic stirrer. The resulting maleinized oleic acid (MOA) was subsequently reacted with both hot water and dilute sodium hydroxide (NaOH, 0.1M). Both hot water and dilute sodium hydroxide were able to fully disperse MOA onto aqueous phase, indicating the successful of hydrolysis of succinic anhydrides ring that yield hydrophilic carboxylic acids functional groups. This hydrolysed MOA is denoted as hMOA. The chemical structure of OA, MOA and

hMOA were verified using ^{1}H-NMR performed with a Bruker DPX400 NMR Spectrometer at 400MHz. The ^{1}H-NMR spectra of OA, MOA and hMOA are given in **Fig.S2**. The chemical shifts were analysed with the reference to the solvent peak (δ = 7.27 ppm, $CDCl_3$).

Table S1. Summary of the integrated intensity of various signals in OA, MOA and hMOA ^{1}H-NMR spectrum.

Samples	Chemical Shift 'a' (2.30 ppm)	Chemical Shift 'd' (1.96 ppm)	Ratio of maleinized 'd' carbon over 'd' of OA
OA	1.00	1.72	-
MOA	1.00	0.99	56.25%
hMOA	1.00	0.97	55.11%

The ^{1}H-NMR results in **Fig.S2** demonstrated that chemical shift at 1.96 ppm arises from the protons of the un-grafted carbon besides the alkenyl functional group still exists on the ^{1}H-NMR spectra of MIONPs and hMIONPs. This indicated the possibilities that only one succinic anhydride was grafted at a time, leaving the carbon on the other side of the alkenyl functional groups remains pristine. However, ^{1}H-NMR spectra cannot be used precisely to distinguish such preferred position. This is because the resulting maleinized oleic acid (MOA) and hydrolysed MOA (hMOA) might contained the mixture of all possible adduct products. Nevertheless, the integrated intensity of the ^{1}H-NMR spectrum signal (see **Table S1**) correspond proportionally to the number of the hydrogens that contributed to the signal can be used to compare the relative amount of the presence of certain carbon signal. In this case, the integrated intensity of the proton signal in 'd' carbon (1.96 ppm) of each ^{1}H-NMR spectrum was normalized against the proton signal in 'a' carbon (2.30ppm), since both 'a' and 'd' carbon carry one proton each. The comparison of such normalized intensity of 'd' carbon signal in MOA and hMOA against the 'd' carbon signal from OA showed that more than 50% of 'd' carbon still remained after the malenization and the hydrolysis processes. Although this indicates that the maleinization process occurred as such 'd' or 'f' carbons of the oleic acid were grafted with succinic anhydride functional groups and the reaction was indeed not 100% completed.

The chemical shifts for pure oleic acid (OA). ^{1}H-NMR (400 MHz, $CDCl_3$) δ: 5.25-5.5 (-HC=CH-), 2.25-2.5 (-CH_2-COOH), 1.9-2.25 (-HC=CH-CH_2-CH_2-), 1.57-1.8 (-CH_2-CH_2-COOH), 1.2-1.55 (-CH_2-CH_2-), 0.8-1.05 (-CH_2-CH_3).

The chemical shifts for maleinized oleic acid (MOA). ^{1}H-NMR (400 MHz, $CDCl_3$) δ: 5.25-5.35 (-HC=CH-), 3.05-3.15 (-O-C(=O)-CH_2-CH-), 2.5-3.0 (-O-C(=O)-CH_2-CH-), 2.15-2.45 (-CH_2-COOH), 1.9-2.05 (-HC=CH-CH_2-CH_2-), 1.5-1.75 (-CH_2-CH_2-COOH), 1.1-1.5 (-CH_2-CH_2-), 0.8-1.0 (-CH_2-CH_3).

The chemical shifts for hydrolysed MOA (hMOA). ^{1}H-NMR (400 MHz, $CDCl_3$) δ: 5.25-5.3 (-HC=CH-), 2.55-2.85 (HOOC-CH_2-CH-COOH), 2.2-2.4 (-CH_2-COOH), 1.85-2.05 (-HC=CH-CH_2-CH_2-), 1.5-1.7 (-CH_2-CH_2-COOH), 1.1-1.5 (-CH_2-CH_2-), 0.8-0.95 (-CH_2-CH_3).

S2. Particle Hydrodynamic Size – DLS Experiment

To further study the size distribution, the hydrodynamic size of hMIONPs in Millipore® water was measured through the dynamic light scattering (DLS) at room temperature (~300K). The measurement was taken three times and the average hydrodynamic size of hMIONPs was found to be 38.8 ± 2.1 nm, as presented in **Fig. S3**.

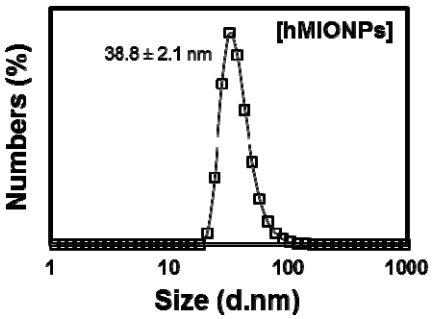

Fig.S3 The hydrodynamic size of hMIONPs in Millipore® water at room temperature 300K. The number-mean average size of hMIONPs recorded from dynamic light scattering experiments (DLS) was 38.8 ± 2.1 nm.

S3. Optimization of the Synthesis of MIONPs

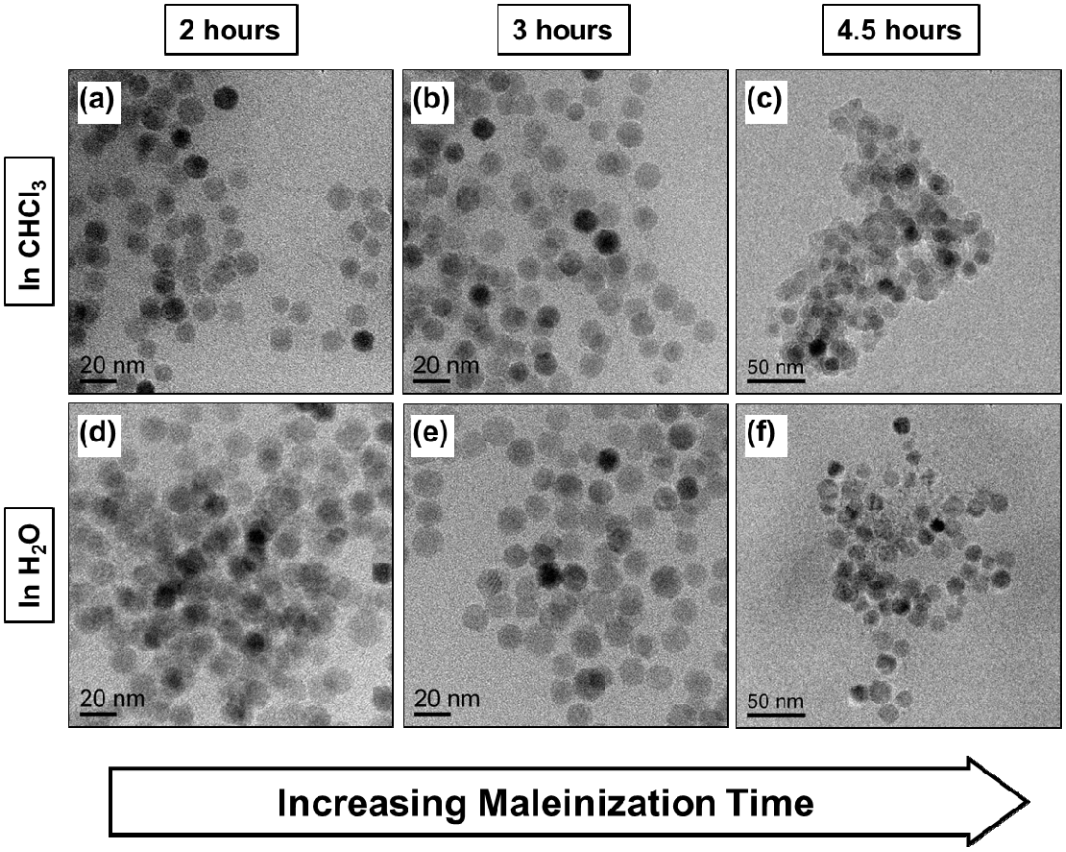

Fig. S4 TEM images of MIONPs in $CHCl_3$ synthesized under different maleinization reaction time: (a) 2 hours, (b) 3 hours and (c) 4.5 hours. The corresponding hMIONPs in water from the MIONPs synthesized under different maleinization reaction time: (d) 2 hours, (e) 3 hours and (f) 4.5 hours.

The attempt to optimize the combinatorial process of maleinization and thermolysis was carried out by by varying the reaction time. Basically, three different maleinization reaction times were employed: (i) 2 hours, (ii) 3 hours and (iii) 4.5 hours (at 210^{o}C). The TEM of the as-synthesized MIONPs were given in **Fig. S4a-c**. From the TEM analysis, it was observed that the prolonged reaction time has no significant effect towards the individual MIONPs crystal size.

When the reaction time was kept at 2 hours, the resulting MIONPs were stable in $CHCl_3$, no aggregation was observed from the TEM images (**Fig. S4a**). The subsequent hydrolysis of the MIONPs onto hMIONPs would result in severe aggregation due to the lack of succinic anhydride functional groups (TEM image of hMIONPs was given in **Fig. S4d**). The lack of the succinic anhydride functional group was caused by the incomplete maleinization process due to the short reaction time. When the maleinization reaction time was increased from 2 hours to 3 hours, the resulting MIONPs were stable in $CHCl_3$ slightly aggregation was observed from the TEM images (**Fig. S4b**). The subsequent hydrolysis yielded a stable hMIONPs solution in water. No significant aggregation was observed from the TEM in **Fig. S4e** as compared to the hMIONPs sample prepared with 2 hours reaction time.

When the maleinization reaction time was elongated from 3 hours to 4.5 hours, the maleinization side/secondary reaction (such as: enophile polymerization, alkenyl functional groups oligomerization, copolymerization between the enophile and alkene and thermal decomposition of the resulting adducts) dominated the overall process [1]. As shown in **Fig. S4c**, the TEM image of the as-synthesized MIONPs nanoparticles in $CHCl_3$ indicated that the nanoparticles were severely polymerized into nanoclusters. Due to its aggregation and large cluster size, the subsequent hydrolysis of such MIONPs would yield an unstable water-dispersible nanoclusters hMIONPs which quickly precipitated after 30 minutes. Similar to the MIONPs, the TEM images of the hMIONPs in **Fig. S4f** after hydrolysis also indicated aggregation problems.

To sum up, in the optimization of the combinatorial process employed in our paper, there were three key findings: (1) the prolonged maleinization reaction time (4.5 hours) would results in large aggregates due to severe side reactions process that occurred, meanwhile (2) too short maleinization reaction time (2 hours) would reduce the aggregations of MIONPs in $CHCl_3$ but the resulting MIONPs were unable to be completely dispersed/transferred into aqueous phase due to lack of the succinic anhydride functional group caused by the low yield (incomplete) of maleinization process. Thus, the intermediate reaction time (3 hours) would be the optimized reaction time due to improved maleinization yield as well as preventing the side reactions to severely occur. The resultant nanoparticles from this optimized process exhibited a good colloidal stability either in $CHCl_3$ or water.

S4. Possible Chain Conformation of MOA and hMOA

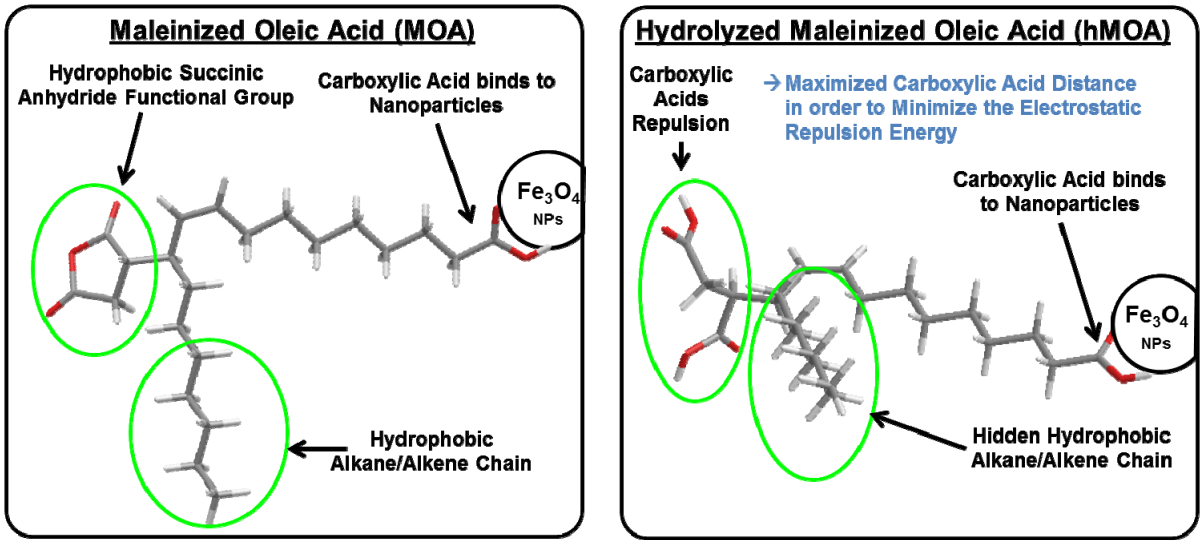

Fig. S5 Possible chemical structure of maleinized oleic acid (MOA) and hydrolyzed MOA (hMOA).

Our as-synthesized nanocrystals would be capped by maleinized oleic acid (from the literature, there are 4 possible configurations for this adduct as shown in **Fig. S1**, one of which is presented in **Fig. S5**). Due to steric repulsion, we believe that the presence of succinic anhydride rings would 'push' the remaining hydrophobic alkane chain away (or alkene, depending on the position of the succinic anhydride). However since both succinic anhydride and alkane/alkene chain are hydrophobic, maleinized oleic acid capped nanocrystals are therefore still soluble in non-polar solvent (e.g. chloroform, $CHCl_3$). As presented in **Fig. S5**, the hydrolysis of the succinic anhydride ring to its analogue hydrophilic succinic acid would add another repulsive force, contributed by the need to maximize the two carboxylic acid distances. In basic aqueous phase, the need to optimize the total energy (maximizing the polar/polar interaction), the hydrophobic alkane/alkene chain is therefore hidden or folded. Although there is no direct evidence, to dissolve back the nanocrystals into non-polar solvent would imply rearrangement of these capping agent configuration (to maximize non-polar/non-polar interaction and minimize non-polar/polar interface) that is thermodynamically unfavorable. Such hydrolyzed maleinized oleic acid 'rigid' configuration would render the nanocrystals insoluble back into non-polar solvent (e.g. chloroform, $CHCl_3$). Therefore, no nanocrystals were observed to reside in the $CHCl_3$/water interface as well as in the $CHCl_3$ phase.

S5. Buffer Stability of Water Dispersible Magnetic Nanoparticles (hMIONPs)

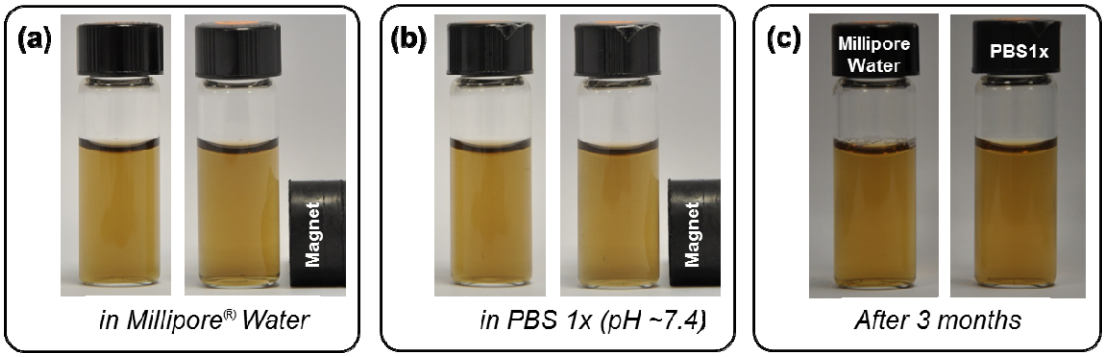

Fig. S6 Digital photograph of (a) hMIONPs in Millipore® water and (b) hMIONPs in phosphate buffered saline solution or PBS 1x (pH ~7.4), both with and without the presence of strong magnetic field (after 1 day incubation with magnetic field). (c) Digital photograph of the same hMIONPs sample in Millipore® water and PBS 1x, taken 3 months after the synthesis (samples are stored in room temperature ~300K).

As illustrated in **Fig. S6**, the hMIONPs solution in both water and PBS 1x appear as transparent brown solution. The incubation with magnetic field over 1-2 days does not result in any significant aggregation or precipitation. The superior colloidal stability attributed to the presence of carboxylic acids functional group on the outer surface that gives both electrostatic and steric repulsion. The colloidal stability of these nanocrystals aqueous solution indicates that the presence of the hydrolysed MOA capping agent is capable to interact with surrounding aqueous medium in order to prevent the aggregation between the nanocrystals. This kind of colloidal stability is superior as compared to those nanocrystals that have been phase transferred and stabilized through ionic/electrostatic repulsion (e.g. tetramethylammonium hydroxide or TMAOH coated nanocrystals) especially in ionic solution such as PBS 1x [4].

S6. FT-IR Spectra of IONPs, MIONPs and hMIONPs

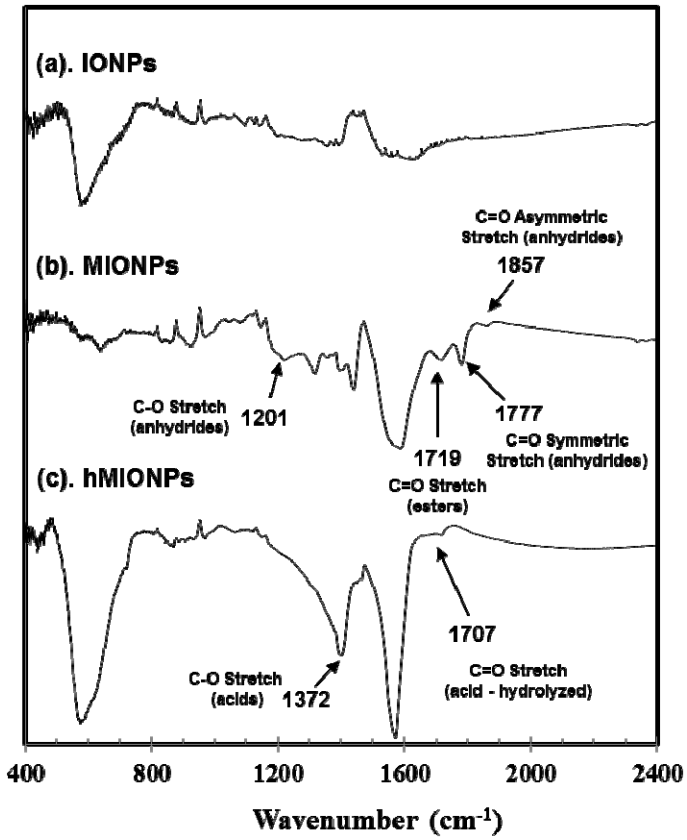

Fig. S7 FT-IR spectra of the powder samples of (a) IONPs, (b) MIONPs and (c) hMIONPs.

The successful grafting of succinic anhydrides onto the oleic acid through maleinization reactions was verified by FT-IR spectroscopy experiment. The characteristics peaks of anhydride in MIONPs are reflected from the absorption at 1777cm^{-1} and 1857cm^{-1} in **Fig. S7b** that corresponds directly to C=O symmetric and asymmetric stretch of anhydrides. Furthermore, the presence of anhydride is also echoed by the presence of the esters C=O stretch peak at 1719cm^{-1} and the anhydrides C-O stretch at 1202cm^{-1} [5]. The hydrolysis of MIONPs would result in the ring opening of succinic anhydride that yield carboxylic acid functional groups which able to stabilize the nanocrystals in aqueous medium. Although the peak for O-H stretch of carboxylic acid are indistinguishable from the peak for C-H stretch in the range of 2400-3400cm^{-1} (data is not shown), the presence of weak carboxylic acid C=O stretch and the carboxylic acid C-O stretch in **Fig. S7c** confirmed the enhancement of the number of carboxylic acids in the hMIONPs.

S7. Thermogravimetric Analysis (TGA) of IONPs, MIONPs and hMIONPs

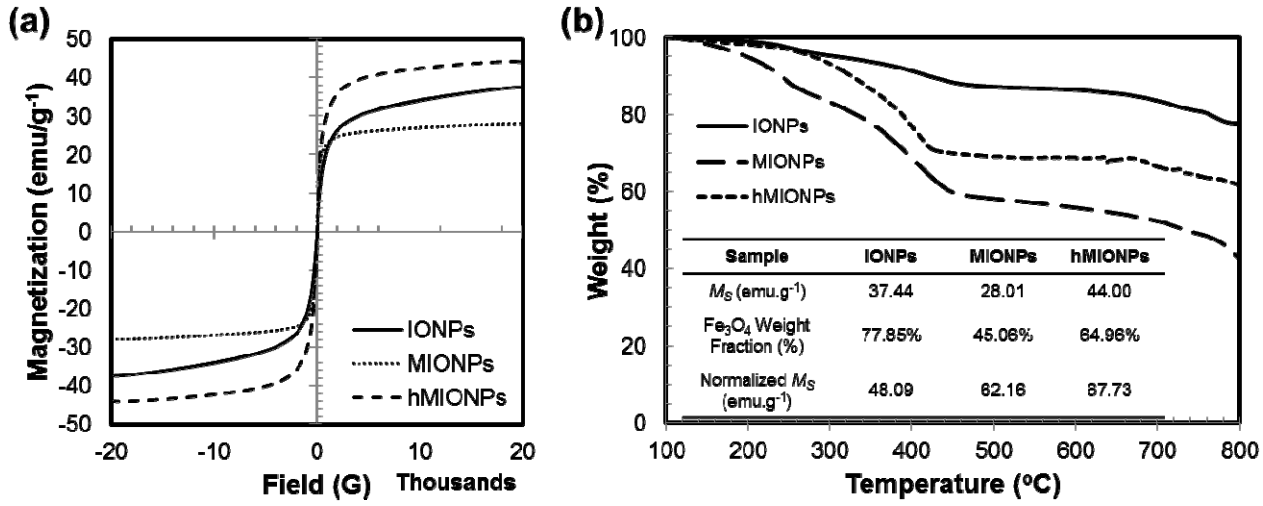

Figure S8. (a) As-measured hysteresis loop profile of IONPs, MIONPs and hMIONPs. (b) Heating profile of IONPs, MIONPs and hMIONPs samples from thermogravimetric analysis (TGA) experiments (inset: a summary table of the original saturation magnetization, Fe_3O_4 weight fraction and the normalized saturation magnetization of IONPs, MIONPs and hMIONPs samples).

The as-measured hysteresis loop profile of IONPs, MIONPs and hMIONPs were given in **Fig. S8a**. The saturation magnetizations were 37.44, 28.01 and 44.00 emu.g^{-1} for IONPs, MIONPs and hMIONPs respectively. The measured saturation magnetization of MIONPs was relatively low as compared to IONPs. One possible reason was the presence of excess maleinized oleic acid capping agents which were required for the water solubilisation of these nanocrystals into aqueous phase. To neglect the surfactant effects, the thermogravimetric analysis (TGA) experiments were performed on IONPs, MIONPs and hMIONPs samples under nitrogen flow (to prevent oxidation of Fe_3O_4 onto Fe_2O_3). The results of the weight loss profile against the temperature were plotted in **Fig. S8b**. The relative Fe_3O_4 weight percentage of IONPs, MIONPs and hMIONPs as compared to the organic surfactant from the TGA results were found to be 77.85%, 45.06% and 64.96% respectively. Our results indeed showed that the low saturation magnetizations of MIONPs were caused by the excessive surfactant coatings. After considering the actual Fe_3O_4 weight percentage, the normalized saturation magnetization of IONPs, MIONPs and hMIONPs neglecting the surfactant effects were found to be 48.09, 62.16 and 67.73 emu.g^{-1} respectively.

S8. Preliminary Study: Water Dispersible Up-Converting Nanocrystals $NaYF_4$:Yb,Er (UCNPs)

In this section, we report our current progress in extending our proposed concept of synthesizing water dispersible nanocrystals. To assess the generality of our proposed concept, we selected up-converting $NaYF_4$:Yb,Er nanocrystals (UCNPs). UCNPs were synthesized through the previously reported protocols [6] with some slight modification to incorporate maleinization process.

Materials:

All the rare-earth trifluoroacetates precursors for the thermolysis synthesis were prepared by reacting each respective rare-earth oxides in trifluoroacetic acid (CF_3COOH) and the resulting rare-earth trifluoroacetates were purified to obtain powder precursors. Sodium trifluoroacetate (CF_3COONa, 98%) and 1-octadecene (technical grade, 90%) were obtained from Aldrich. Oleic acid (OA, ≥99.0%) was purchased from Fluka. Chloroform ($CHCl_3$) was purchased from Fisher Scientific.

Synthesis:

Synthesis of MOA-capped UCNPs. To synthesize the maleinized oleic-acid (MOA) capped NaYF4:20%Yb,2%Er sample, 0.025 mmol of $Er(CF_3COO)_3$ (0.025 mmol, 12.66 mg), $Yb(CF_3COO)_3$ (0.25 mmol, 128.02 mg), $Y(CF_3COO)_3$ (0.975 mmol, 417.25 mg) and sodium trifluoroacetate $Na(CF_3COO)_3$ (1.25 mmol, 170.01 mg) were charged into three-neck round bottom flask. Oleic acid and 1-octadecene (each 10 mL) were added into the flask. The resulting transparent mixture was heated up to 110^{o}C to remove the residual water and oxygen under inert nitrogen gas atmosphere. Under vigorous stirring, the solution was then further heated to 330^{o}C under nitrogen gas flow and maintained at this temperature for 1 hour. The mixture was allowed to cool down to 210^{o}C and maleic anhydride (64 mmol, 6.28 grams) was injected to the solution mixture. The yellow solution would turn into brown colour solution. The reaction was allowed to proceed for another 3 hours in static nitrogen atmosphere. The resulting reddish brown mixture were precipitated by the addition of ethanol and isolated by using centrifugation at 8000rpm for 5 minutes. The resulting nanoparticles (denoted as **MOA-UCNPs**) were washed once more time with ethanol. The resulting precipitates were dispersed in $CHCl_3$ and stored in a sealed glass vial.

Converting MOA-capped UCNPs into hMOA-capped UCNPs. To obtain water soluble UCNPs, MOA-UCNPs were precipitated by ethanol addition and isolated by centrifugation at 8000rpm for 5 minutes. To the resulting precipitates, dilute sodium hydroxide (NaOH, 0.1M) was added and the mixture was sonificated in ultrasonic bath for 10-15 minutes at 60^{o}C. The final product was hMOA capped nanocrystals was purified and dispersed back into aqueous phase (denoted by **hMOA-UCNPs**). The final solution colour is light brown. The brown colour solution of UCNPs could be the result of the slight colour change that was previously reported to occur during prolonged heating at elevated temperature [7].

Reference

[1]. (a) F. Stefanoiu, L. Candy, C. Vaca-Garcia, E. Borredon, *European Journal of Lipid Science and Technology* **2008**, *110*, 441-447. (b) J. o. Metzger, U. Biermann, *Lipid / Fett* **1994**, *96*, 321-323. (c) L. Candy, C. Vaca-Garcia, E. Borredon, *European Journal of Lipid Science and Technology* **2005**, *107*, 3-11. (d) L. Candy, C. Vaca-Garcia, E. Borredon, *Journal of the American Oil Chemists' Society* **2005**, *82*, 271-277.

[2]. W. Bickford, P. Krauczunas, D. Wheeler, *Journal of the American Oil Chemists' Society* **1942**, *19*, 23-27.

[3]. A. Behr, H. P. Handwerk, *Lipid / Fett* **1992**, *94*, 204-208.

[4]. M. Liong, H. Shao, J. B. Haun, H. Lee, R. Weissleder, *Advanced Materials* **2010**, *22*, 5168-5172.

[5]. (a) G. M. O. Barra, J. S. Crespo, J. R. Bertolino, V. Soldi, A. T. N. Pires, *Journal of the Brazilian Chemical Society* **1999**, *10*, 31-34. (b) G.-C. Chitanu, L.-I. Zaharia, A. Carpov, *International Journal of Polymer Analysis and Characterization* **1997**, *4*, 1-20.

[6]. (a) G. S. Yi, G. M. Chow, *Advanced Functional Materials* **2006**, *16*, 2324-2329. (b) J.-C. Boyer, F. Vetrone, L. A. Cuccia, J. A. Capobianco, *Journal of the American Chemical Society* **2006**, *128*, 7444-7445. (c) J.-C. Boyer, L. A. Cuccia, J. A. Capobianco, *Nano Letters* **2007**, *7*, 847-852.

[7]. S. Lin, A. Hsieh, D. Min, S. Chang, *Journal of the American Oil Chemists' Society* **1976**, *53*, 157-161.